

## Forecasting saltwater intrusion volume and sulfate content in a wastewater collection system. Case study: Barreiro/Moita WWTP, Portugal

A. Figueiredo <sup>a,\*</sup>, L. Amaral <sup>b</sup> and J. Pacheco<sup>c</sup>

<sup>a</sup> Department of Environmental Sciences and Engineering, NOVA School of Science and Technology, NOVA University of Lisbon, Quinta da Torre, 2829–516 Monte de Caparica, Portugal

<sup>b</sup> CENSE, Center for Environmental and Sustainability Research, NOVA School of Science and Technology, NOVA University of Lisbon, Quinta da Torre, 2829–516 Monte de Caparica, Portugal

<sup>c</sup> SIMARSUL – Saneamento da Península de Setúbal, S.A., Barreiro/Moita WWTP, 2835–351 Lavradio Barreiro, Portugal

\*Corresponding author. E-mail: agv.figueiredo@campus.fct.unl.pt

 AF, 0000-0002-6170-2060; LA, 0000-0003-1125-1764

### ABSTRACT

The presence of salt water from the Tagus Estuary has been identified in the influent at Barreiro/Moita Wastewater Treatment Plant (WWTP), Portugal. The intrusion occurs throughout damaged sections and direct vectors in the wastewater collection system, during high tide levels, changing the wastewater characteristics and impacting the WWTP process. This study designed models to quantify this problem, enabling more effective countermeasures within the right timing. The proposed models estimate the average volume of salt water and sulfate ( $\text{SO}_4^{2-}$ ) load for each high tide period. The laboratory results show strong correlations between the influent electrical conductivity (EC) and percentage of salt water in WWTP inflow (0.9909), and between EC and  $\text{SO}_4^{2-}$  concentration in WWTP influent (0.9797). The forecast models also show good correlation between the high tide levels with volume of salt water (0.9145) and  $\text{SO}_4^{2-}$  load (0.9162) entering the system. Considering the total monthly inflow, the highest percentage of salt water registered in WWTP inflow was 3.6%. During high tide periods, critical situations have been assessed with up to 53.9% of salt water in the WWTP inflow, increasing energy consumption and costs in pumping stations.

**Key words:** electrical conductivity, forecasting models, saltwater intrusion, undue inflow, wastewater collection system, wastewater treatment plant (WWTP)

### HIGHLIGHTS

- Assessment methodology to quantify saltwater volume and sulfate load from saltwater intrusion in wastewater collection systems.
- Saltwater intrusion impacts on WWTP process.
- Forecast tools for WWTP management teams.

### INTRODUCTION

Around the globe most communities are located in coastal areas making their main wastewater treatment collection systems and treatment plants to preferably be located at the lowest areas, taking advantage of the gravity flow. At the Barreiro/Moita Wastewater Treatment Plant (WWTP), located in Portugal, the presence of salt water from the nearby Tagus Estuary has been identified in the wastewater inflow. The saltwater intrusion effects are clearly detected during periods of high tides in the estuary. Similar issues have been identified in other wastewater collection systems and WWTPs (Serrano 2014; Phillips *et al.* 2015). This problem may occur throughout old and/or damaged sections, joints, manholes, emergency overflow weirs' discharge sites from separated and/or combined wastewater and stormwater collection systems, and also, pumping stations' emergency overflow weirs. Some of the emergency overflow weirs' discharge channels are equipped with retention valves that might not always work properly, and, in other cases, they are not installed, making these sites direct vectors for salt water entering into the collection systems. Due to the unexpected and unwanted presence in the wastewater flow of saltwater volume, the saltwater intrusion in these wastewater collection systems is considered an undue inflow.

This is an Open Access article distributed under the terms of the Creative Commons Attribution Licence (CC BY 4.0), which permits copying, adaptation and redistribution, provided the original work is properly cited (<http://creativecommons.org/licenses/by/4.0/>).

Saltwater intrusion into wastewater collection systems causes extensive structural damage, increasing maintenance costs (Phillips *et al.* 2015). One of the main causes of structural damage to steel and concrete structures in these systems is sulfuric acid ( $\text{H}_2\text{SO}_4$ ), which is generated by the oxidation of hydrogen sulfide ( $\text{H}_2\text{S}$ ). The  $\text{H}_2\text{S}$  arises from sulfate ( $\text{SO}_4^{2-}$ ) reduction by sulfate-reducing bacteria (Zhang *et al.* 2008) present in these systems. The increase in  $\text{SO}_4^{2-}$  load in the wastewater, due to saltwater intrusion, intensifies the problem and its consequences.

Widely recognized and recommended is the need to prevent and assess saltwater intrusion impacts upstream along the wastewater collection system rather than downstream within WWTP processes (Firer *et al.* 2008; Zhang *et al.* 2008; Talaie-khozani *et al.* 2016). To help this assessment it is considered good practice to develop accurate mapping of the collection system network and pumping stations, and locate the most critical saltwater intrusion sites (Phillips *et al.* 2015; Talaiekhazani *et al.* 2016).

Saltwater intrusion affects WWTP processes by changing the wastewater characteristics (Metcalf & Eddy 2014). The wide variety of high tide levels during tide cycles in the estuary and the degree of saltwater intrusion severity make it difficult to apply successful countermeasures. The process and corrective actions can be improved by using forecasting models that enable quantification of the extra volume and loading components. With a viable forecasting model methodology, it is possible to time countermeasures properly, anticipating and attenuating impacts downstream at the WWTP. Once established and consolidated, such models will enable quantification of this undue inflow and assess the economic damage caused by increased energy consumption in pumping stations from both systems, wastewater collection systems and WWTPs.

Analysis of the tide level time series from the Cascais mareograph near the Tagus Estuary demonstrates a mean sea level rise of  $2.20 \text{ mm}\cdot\text{year}^{-1}$  between 1999 and 2004, and  $4.10 \text{ mm}\cdot\text{year}^{-1}$  between 2005 and 2016 (Antunes 2016). It is expected that, with the mean sea level rise caused by climate change, it will increase tide levels in the estuary, intensifying the saltwater volume entering into the wastewater collection system and, therefore, into the WWTP, increasing negative impacts of this undue inflow in processes.

The aim of this study is to develop a forecasting model based on high tide values, to provide measurable quantification of saltwater intrusion's volume and  $\text{SO}_4^{2-}$  load, to help WWTP management teams to apply better countermeasures within the right timing. It will also enable the understanding and assessment of the extent of economic impacts on the water utility caused by this undue inflow.

### Wastewater collection system and WWTP process characterization

The study was carried out in Barreiro/Moita WWTP combined wastewater and stormwater collection systems, which receive urban and industrial wastewater, and stormwater. The main network interceptor sections are located along Barreiro and Moita municipalities' coast line with the Tagus Estuary. Some sections are old and mainly placed below mean Tagus Estuary water level, facilitating saltwater intrusion into the collection system's underground network. The main collection system interceptors collect wastewater from smaller nearby collection system networks managed by inherent municipalities and industrial zones. The wastewater collection system, including its pumping stations and the WWTP, is managed by the local water utility, SIMARSUL (Saneamento da Península de Setúbal, S.A.) (Figure 1).

The Barreiro/Moita WWTP has a maximum treatment capacity of up to 300,000 p.e. (population equivalent) and comprises the following treatment processes: initial pumping station, pre-treatment, primary treatment with lamella plate settlers, followed by conventional aeration, ending with ultra-violet (UV) radiation disinfection prior to treated water final discharge. Primary sludge is gravity-thickened, and waste biological sludge is thickened by mechanical rotary drums. The thickened sludges are mixed and stabilized by anaerobic digestion, before dewatering by centrifuge, being later valued properly as biosolids. Also, there is an extra stormwater chemically advanced primary treatment parallel line.

### Saltwater impacts and countermeasures

The presence of salt water in the wastewater increases the  $\text{SO}_4^{2-}$  content leading to generation of odor in the wastewater collection system. These odors are attributed to the presence of  $\text{H}_2\text{S}$  formed by the action of anaerobic bacteria in the system wall's biofilm. These anaerobic sulfate-reducing bacteria (e.g., *Desulfovibrio*) reduce  $\text{SO}_4^{2-}$  present in wastewater to  $\text{H}_2\text{S}$  (McGhee 1991). The increase in  $\text{H}_2\text{S}$  concentration in a system infrastructure's atmosphere is responsible for corrosion, and potentiates harm to operation and maintenance workers' health (Firer *et al.* 2008). Corrosion is caused by acidification due to the oxidation of  $\text{H}_2\text{S}$  to form  $\text{H}_2\text{SO}_4$ , typically by the action of *Thiobacillus* present in the biofilm fixed on the pipe section's top walls (McGhee 1991), or through side reactions with water ( $\text{H}_2\text{O}$ ) condensation. For this oxidation process

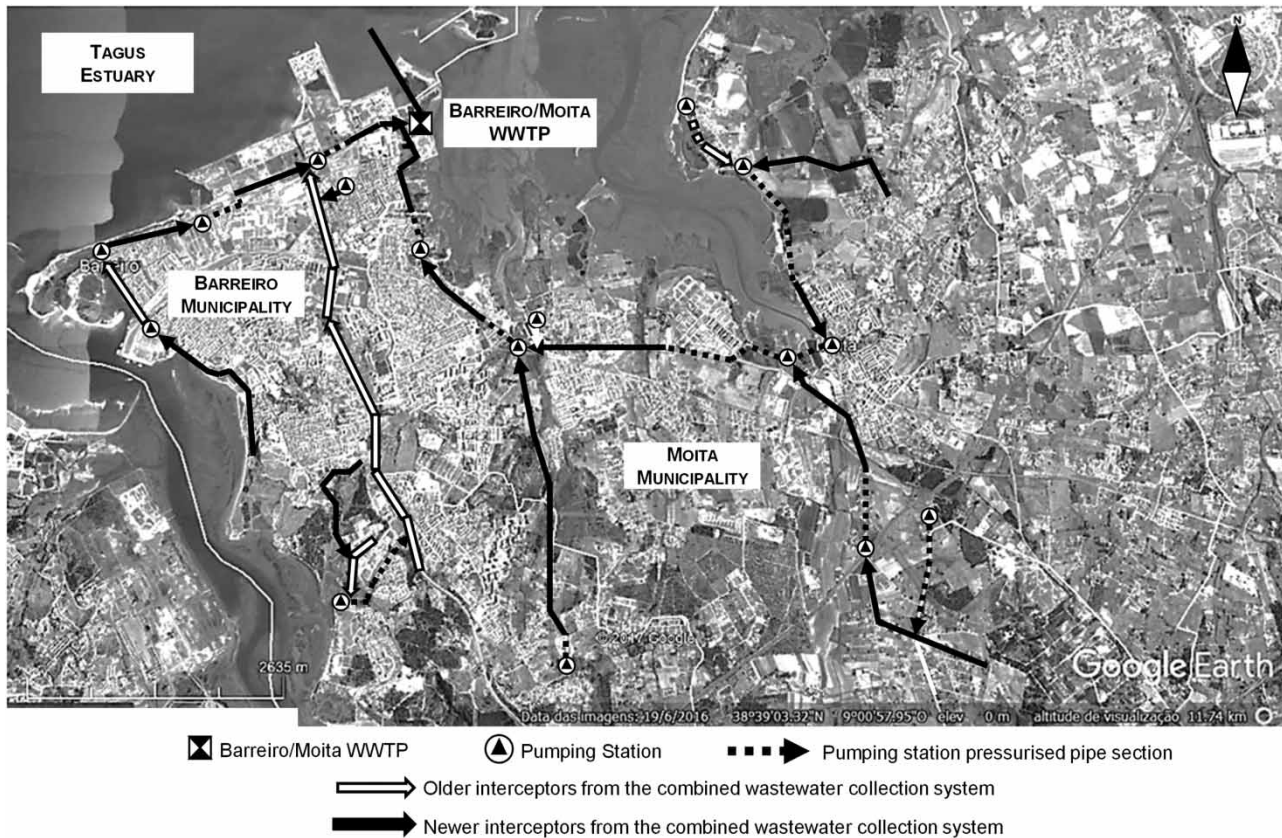


**Figure 1** | Main interceptors and pumping stations in Barreiro/Moita's WWTP wastewater collection system.

to occur low oxygen concentration in the system's atmosphere is required. The corrosion caused by  $\text{H}_2\text{SO}_4$  can reduce the thickness of concrete pipe sections' top wall by 1 to 10  $\text{mm}\cdot\text{year}^{-1}$ , generating additional costs for water utilities (Zhang *et al.* 2008) for maintenance and rehabilitation needs.

The main changes in wastewater influent characteristics are in its density, temperature, constituent loadings (e.g., chlorides ( $\text{Cl}^-$ ) and ( $\text{SO}_4^{2-}$ ) and volume, all of which affect different WWTP processes with the possibility of compromising the final treated water quality and regulatory compliance. Changes in density and temperature can cause stratification in primary settlers, leading to a decrease in solids' retention and process efficiency. Stratification leads to the accumulation of denser and colder salt water in the bottom of primary settlers, increasing saltwater constituent concentrations (i.e.,  $\text{SO}_4^{2-}$ ) in primary sludges.

A significant impact of saltwater intrusion arises during sludge anaerobic stabilization in digesters. The primary and biological thickened sludges each represent about 50% (1:1 ratio) of the digester feed, but the main  $\text{SO}_4^{2-}$  contributor is the primary thickened sludge assessed by its higher electrical conductivity (EC) values. Excess  $\text{SO}_4^{2-}$  in thickened sludge leads to higher  $\text{H}_2\text{S}$  content in biogas generated. The cogeneration system that uses the biogas stops when the maximum allowed  $\text{H}_2\text{S}$  value is exceeded, ceasing both energy generation and heat recovery, lowering the anaerobic digester's temperature. These factors cause difficulties in keeping the anaerobic digestion process stable and efficient. The registered time series datasets from the WWTP enable a correlation to be observed between maximum tide levels in high tide cycles and high  $\text{H}_2\text{S}$  content in biogas. The sinusoidal behavior of the two variables is similar and the peak values show a constant pattern of 5 to 7 days' delay between the cycle maximum high tide level and the peak  $\text{H}_2\text{S}$  concentration in biogas. This delay is attributed to the digester's hydraulic retention time of 10 to 14 days, which gradually accumulates  $\text{SO}_4^{2-}$ , maintaining a complete mix state providing stable inertia that justifies the delay. Some of the buildup  $\text{SO}_4^{2-}$  is reduced into  $\text{H}_2\text{S}$  in solution, which is transferred to a gaseous phase – biogas – causing the problems mentioned in the cogeneration process.

The impact in WWTP processes has been currently attenuated by dosing ferric chloride ( $\text{FeCl}_3$ ) in the plant's headworks during its pre-treatment stage. This strategy has some benefits including the reduction of the organic load into the aeration

tanks and lowering the biogas's  $\text{H}_2\text{S}$  concentration through ferrous sulfide ( $\text{FeS}$ ) precipitation. The main problem is that tide level variation is highly dynamic. Such variation leads to different saltwater intrusion volumes and  $\text{SO}_4^{2-}$  loads, which need to be quantified and managed accordingly for an efficient chemical dosage. Local high tide values used for forecasting are forecasted and provided by the Portuguese Instituto Hidrográfico (IH) (Hydrographic Institute). The forecasting, for instance, will assist decision-making on  $\text{FeCl}_3$  dosage to be applied during different tide cycles in the Tagus Estuary.

## MATERIALS AND METHODS

### Tagus Estuary tide level time series dataset

Tide levels in the Tagus Estuary can be obtained from forecasts on the IH website, which shows high and low tide levels, the day, hour and minute of occurrence, in this case for Lisbon Harbor. These data enable determination of the consecutive tide levels between low and high tides (IH 2017) (see Figure 2). The mathematical expressions provided by IH are presented below.

Equation (1) enables calculation of tide level,  $y$  (m), at any time between high tide and the next low tide:

$$y = \frac{H+h}{2} + \frac{H-h}{2} \times \cos\left(\frac{\pi \times t}{T}\right) \quad (1)$$

where  $y$  is the tide level (m) between a given high tide ( $H$ ) level (m) and a low tide ( $h$ ) level (m) at a specific time ( $t$ ) (min) within the total time ( $T$ ) (min) from high to low tide level.

Equation (2) enables calculation of tide level,  $y_1$  (m), at any time between low tide and the next high tide:

$$y_1 = \frac{h+H_1}{2} + \frac{h-H_1}{2} \times \cos\left(\frac{\pi \times t_1}{T_1}\right) \quad (2)$$

where  $y_1$  is the tide level (m) between a given low tide ( $h$ ) level (m) and a high tide ( $H_1$ ) level (m) at a specific time ( $t_1$ ) (min) within the total time ( $T_1$ ) (min) from low to high tide level.

It is, thus, possible to generate a continuous time series dataset of tide levels covering the study period.

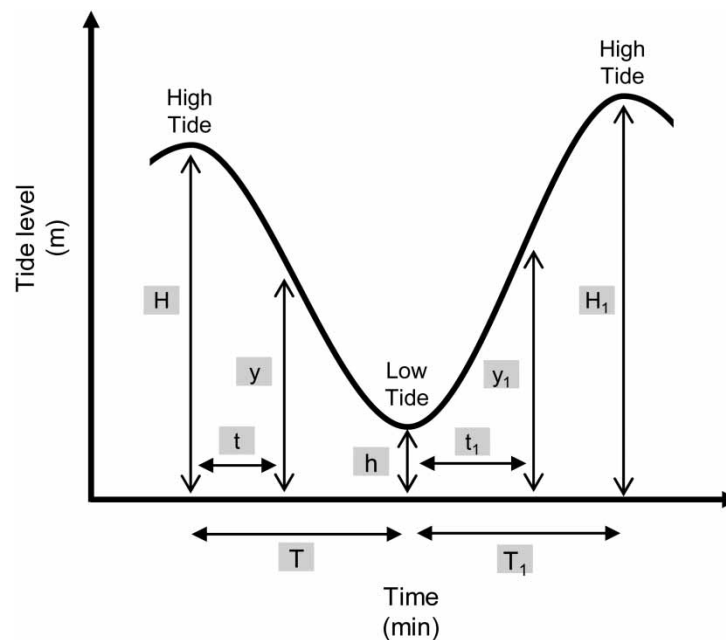


**Figure 2** | Tide level variables (adapted from IH 2017).

### Assessment of EC in the Tagus Estuary near the WWTP

The presence of salt water in WWTP influent can be detected by measuring its EC (APHA 1999; Serrano 2014). The EC of water depends on temperature and, for a typical urban wastewater, is between 680 and 2,038  $\mu\text{S}\cdot\text{cm}^{-1}$  at 20 °C (Metcalf & Eddy 2014). The EC of water from the Atlantic Ocean generally exceeds 40,000  $\mu\text{S}\cdot\text{cm}^{-1}$  at temperatures above 10 °C (Degrémont 1989).

The EC values in the Tagus Estuary near the wastewater collection system were taken from time series datasets from floating water quality stations nearby in the Tagus Estuary (SNIRH/APA). The location of the water quality stations is represented in Figure 3 and their respective EC values summarized in Table 1. The minimum and maximum EC values were assessed for each station's time series dataset and the arithmetic mean calculated for the general minimum and maximum, to obtain an expected EC range for the study area. The results comply with the tidal water movements expected in that part of the estuary, for instance, high EC levels at high tide due to incoming salt water from the Atlantic Ocean through the south side, and lower values at low tide, when ocean water returns and is replaced by less salty waters from the Tagus Estuary and other fresh water sources nearby.

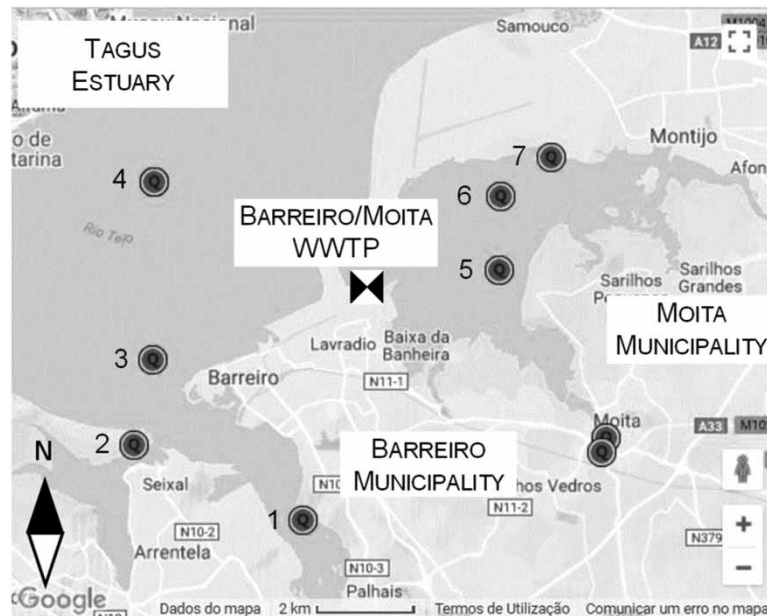


**Figure 3** | Local floating water quality stations in the Tagus Estuary, Portugal (source: SNIRH 2017).

**Table 1** | Floating water quality station EC values for the Tagus Estuary (period of record 1999 to 2005)

Water quality station ID		EC ( $\mu\text{S}\cdot\text{cm}^{-1}$ )	
		Minimum	Maximum
1	ESTEIRO COINA (22C/05)	25,240	44,460
2	ESTEIRO SEIXAL (22C/06)	29,560	45,010
3	TEJO – BÓIA 14B – CANAL BARREIRO (22C/25S)	–	–
4	TEJO – WB1 – A (S) (21C/11S)	–	–
5	ESTEIRO MOITA (21C/06)	30,210	45,840
6	TEJO – ESTEIRO MOITA/MONTIJO (21C/10)	–	–
7	ESTEIRO MONTIJO (21C/07)	28,730	45,260
<b>General arithmetic mean</b>		28,435	45,143

### Quantifying the percentage of salt water in WWTP inflow measuring EC

The WWTP influent's EC increases continuously as salt water enters the wastewater collection system. To assess the relationship between WWTP influent's EC and percentage (%) of salt water in the inflow it is necessary to perform laboratory tests. The wastewater samples must be taken while salt water is not entering the collection system network due to high tide levels (i.e., during the transitional period between low and high tide), when the influent's EC values should be near, or below,  $2,000 \mu\text{S}\cdot\text{cm}^{-1}$ . The saltwater samples should be collected during the high tide peak level along the coastal area near wastewater collection system infrastructures. The wastewater and saltwater samples should be at room temperature ( $20^\circ\text{C}$ ) and mixed in 1 L beakers accordingly to meet their respective percentages of salt water in volume (e.g., 0%, 10%, 20%, etc.). The resulting solutions are mixed in a jar-test equipment, or an electromagnetic stirrer, at 120 rpm for 2 min ensuring good mixture thus avoiding any possible stratification, before the solution's EC is measured.

The expected correlation between the influent's EC and percentage of salt water in the WWTP inflow will be similar to a straight line starting at the base line for the expected wastewater EC (see Figure 4). However, it is necessary to be cautious when analyzing the results for mixtures containing high percentages of salt water in terms of flow dynamics in wastewater collection systems. Normally, in the main interceptors wastewater will always be flowing, and it will be difficult to achieve mixtures with high percentages of salt water. Therefore, the high percentage values will generate a slightly curved and uncertain end line. This method is suitable for low to medium percentages of saltwater values, but not recommended for higher values without any thorough concerns.

Having determined this correlation, the percentage of salt water in the WWTP inflow can be estimated from the influent's EC, enabling the quantification of the volume of salt water in the WWTP inflow from the influent's EC and inflow time series datasets.

### Quantifying the saltwater sulfate concentration in WWTP influent by measuring EC

The  $\text{SO}_4^{2-}$  load is important for the countermeasures to manage saltwater impacts in the WWTP processes, as well as future WWTP mass balance assessments and strategies. The method used is very similar to the one described above, and both should be done simultaneously, ensuring that the EC, percentage of salt water, and  $\text{SO}_4^{2-}$  concentration are values measured from the same test solutions. The expected graphical representation is shown in Figure 5.

The correlation found enables estimation of the additional  $\text{SO}_4^{2-}$  load from the salt water in the WWTP inflow based on the EC time series dataset.

### Forecast models based on correlation between the Tagus Estuary tide levels, and WWTP influent's EC, volume of salt water, and sulfate load in the influent

High tide levels in the Tagus Estuary are correlated significantly with saltwater intrusion into the Barreiro/Moita WWTP wastewater collection system. Tide levels can be predicted using the IH tool noted above. The tide level time series dataset is associated with the WWTP inflow and headwork influent's EC time series dataset. Missing data from the WWTP inflow are adjusted using the corresponding hourly average inflow (specific for weekday, holiday, or weekend pattern). Missing influent's EC data cannot be adjusted. With the final time series dataset established, the groundwork has been created for the forecasting models.

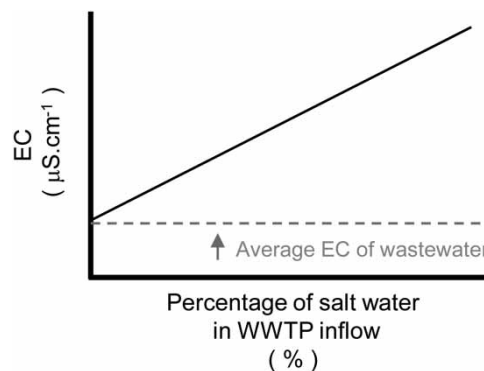


**Figure 4** | Expected scatterplot regression line between EC and percentage of salt water in WWTP inflow.

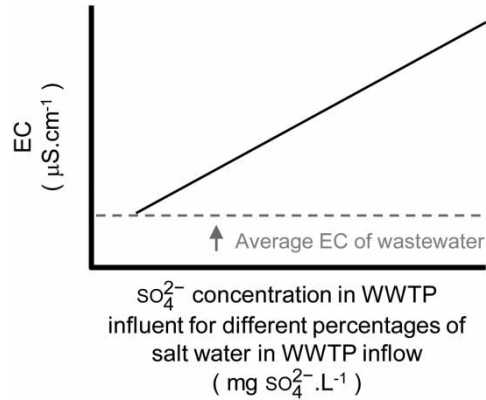


**Figure 5** | Expected regression line between EC and sulfate concentration in the WWTP influent.

The regression lines obtained from the laboratory work, previously described, will be applied to the initial influent's EC time series dataset providing two new time series datasets with the percentage of salt water in the WWTP inflow and  $\text{SO}_4^{2-}$  concentration in WWTP influent. The methodology is only applied on EC values higher than, approximately,  $2,000 \mu\text{S}\cdot\text{cm}^{-1}$ . For lower EC values, it is assumed that saltwater intrusion is not occurring in the wastewater collection system.

The next step of the procedure consists of computation of two more time series datasets that will contain the saltwater volume and  $\text{SO}_4^{2-}$  load values, which are calculated based on three time series datasets: percentage of salt water in WWTP inflow,  $\text{SO}_4^{2-}$  concentration in WWTP influent, and WWTP inflow.

To set up the models, the period between two consecutive high tides is assessed. Then, integrated values of saltwater volume and  $\text{SO}_4^{2-}$  load are attributed to the period's first high tide level. The relationships between high tides, periods, and influent's EC correlated variables are shown in Figure 6.

Each period's high tide will correspond to a different volume of salt water and  $\text{SO}_4^{2-}$  load values, even similar ones, because each period will have a different duration and the WWTP inflow changes during the day, affecting its capacity to dilute salt water. In this time series dataset analysis, it can be noticed that there is a partial lag of variables' synchronization; the small

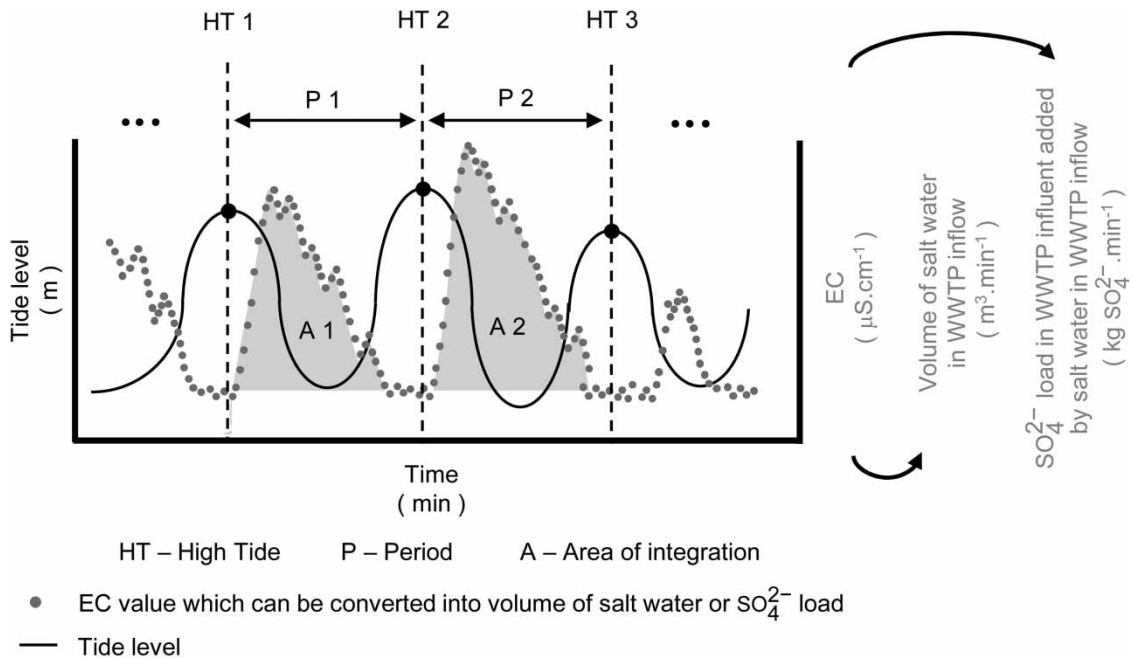


**Figure 6** | High tide level and period correlation, with integration areas for volume of salt water and  $\text{SO}_4^{2-}$  load.

oscillations verified between tide levels and influent's EC arise and are caused by the delays in the wastewater collection network's pumping stations and the network's hydraulic retention time.

The next step is to generate a dataset of the periods' high tide levels selected without any replicates. Then, for each high tide level, the correspondent average values of the volume of salt water and  $\text{SO}_4^{2-}$  load from the time series dataset that contain the data are calculated: period identification, period correspondent high tide level, and the integrated values of saltwater volume and  $\text{SO}_4^{2-}$  load for each period. The dataset generated enables the determination of regression curves that correlate high tide level values with average volume of salt water in the WWTP inflow and  $\text{SO}_4^{2-}$  load in WWTP influent (see Figure 7).

## Materials

The influent EC, at the WWTP, was measured using a field probe (Endress+Hauser Indumax CLS50D) in the headworks channel, after the initial pumping station and before any chemical dosage ( $\text{FeCl}_3$ ). The EC recorded was corrected to a standard temperature of 20 °C and data stored in a data logger.

The laboratory work was conducted using standard and certified laboratory equipment. EC in the laboratory was measured with a Skalar SP50 multi-sample analyzer and  $\text{SO}_4^{2-}$  was determined using a Hach Lange DR 3,900 spectrophotometer with Hach Lange Kit TNT 864 [40–150] mg  $\text{SO}_4^{2-} \cdot \text{L}^{-1}$ , which complies with APHA (1999) standards. For values outside the kit's range, samples with lower volume were diluted with deionized water.

## RESULTS AND DISCUSSION

### Correlation between EC and percentage of salt water in WWTP inflow

The relationship determined in the laboratory tests between EC and the percentage of salt water in the WWTP inflow (%) is shown in Figure 8 (error bars for 95% significance).

It is noted that the WWTP influent's EC value, when saltwater intrusion was not occurring (i.e., intrusion was 0%), was  $2,346 \mu\text{S} \cdot \text{cm}^{-1}$ , which is consistent with field measurements. The results showed a linear behavior as expected. For the 100% value the approximately  $40,000 \mu\text{S} \cdot \text{cm}^{-1}$  value can be seen to be compliant with the expected EC values' interval if the WWTP influent was 100% of salt water from the Tagus Estuary (see Table 1), which, as mentioned before, will not be a real possibility in normal conditions, thus there will always be wastewater flowing through the main interceptors.

### Correlation between EC and $\text{SO}_4^{2-}$ concentration in WWTP influent

As mentioned above, the correlation determined in the laboratory tests between EC and  $\text{SO}_4^{2-}$  concentration was strong. The scatterplot is shown in Figure 9 (error bars for 95% significance).

The lowest  $\text{SO}_4^{2-}$  concentration found was  $79.5 \text{ mg } \text{SO}_4^{2-} \cdot \text{L}^{-1}$  (0%), which is normal for wastewaters not affected by saltwater intrusion, but it is a low value compared with this specific WWTP influent's  $\text{SO}_4^{2-}$  concentration time series dataset, due to the non-correlation between the plant laboratory's sampling plan and the timing of saltwater intrusion into the wastewater collection system. Samples are always collected at the same time and place, regardless of the tide level in the Tagus Estuary and the subsequent presence of salt water in the influent due to saltwater intrusion.

### Forecasting model results and data analysis

The time series dataset for the assessed period was evaluated alongside the forecasting model design process. The monthly time series data assessment comprised the maximum high tide level, the maximum instantaneous percentage of salt water in WWTP inflow, the estimated saltwater volume entering the wastewater collection system and its relative percentage to total WWTP inflow (Table 2). The saltwater volume estimation, determined by integrating saltwater volumes from the time series, might show minor deviations caused by small missing influent EC data, that cannot be adjusted.

Although the saltwater intrusion volumes into the wastewater collection system seem low, compared with the monthly WWTP inflow, their impact on various WWTP processes are very significant. Specific instances can give some idea of the dimension of the problem, such as, on 27 April 2017, at 04:40 in the morning, there was a 4.16 m high tide in the Tagus Estuary and later on at 06:56 the percentage of salt water in the WWTP inflow reached a maximum of 53.9%. As a result, during some period of time in that morning, the pumping stations were moving approximately twice the expected wastewater volume, representing significant additional energy consumption and operating costs.

The forecasting models created show strong correlations and will enable an expeditious estimation of both volume of salt water and  $\text{SO}_4^{2-}$  load, related to high tide level (see Figures 10 and 11).

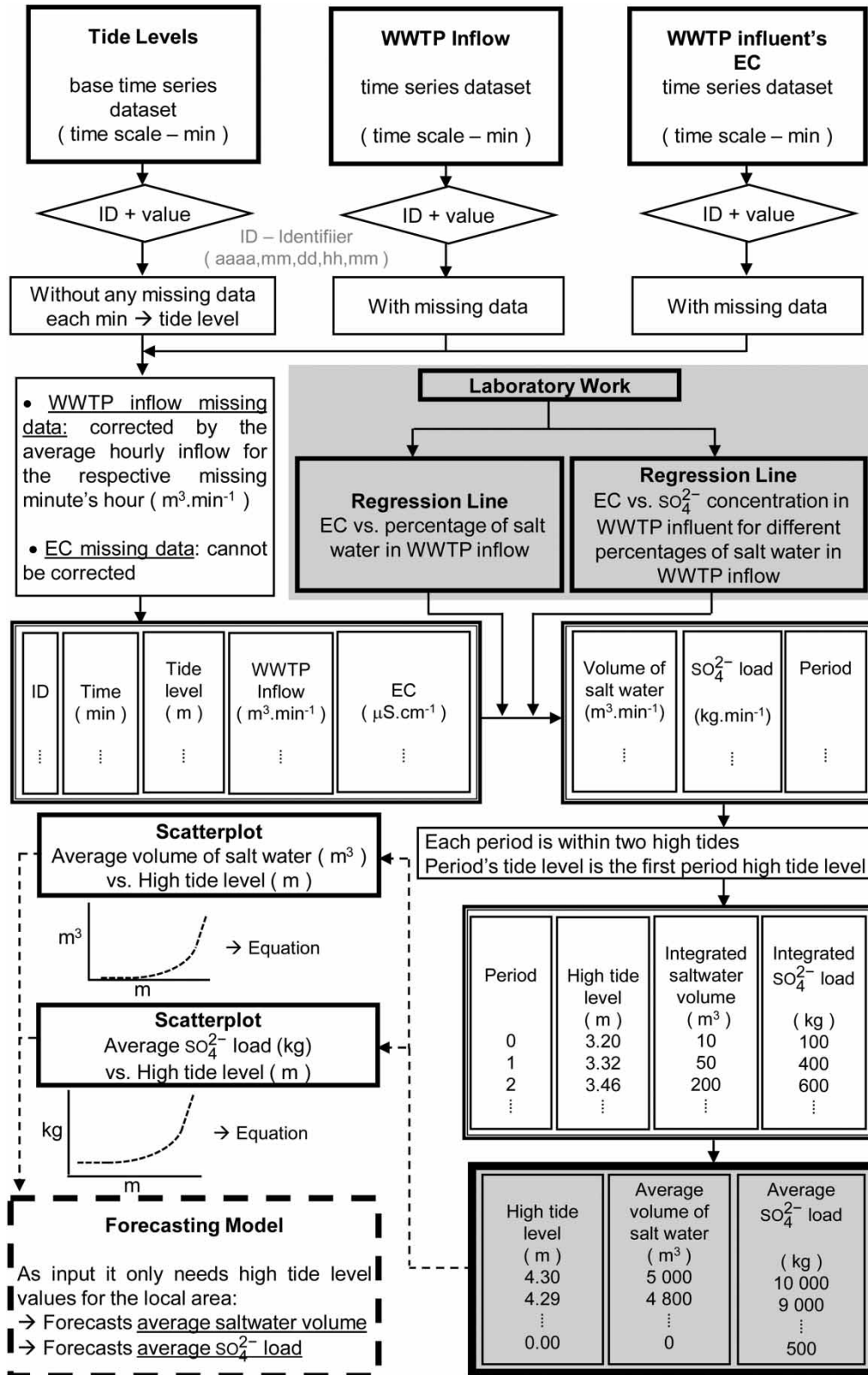
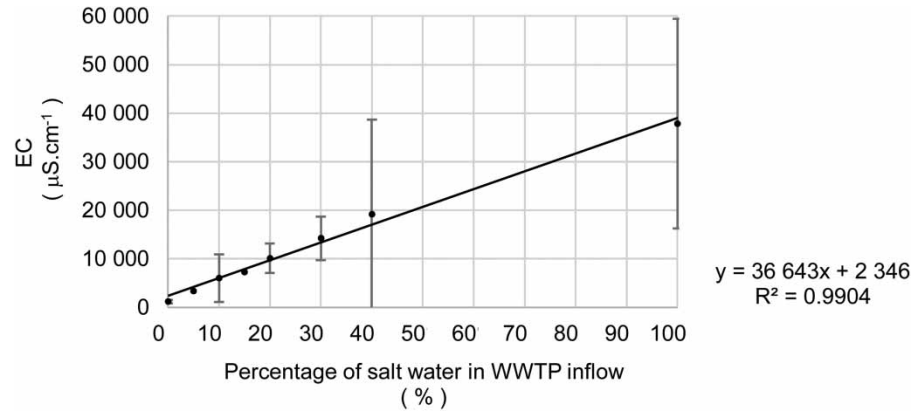
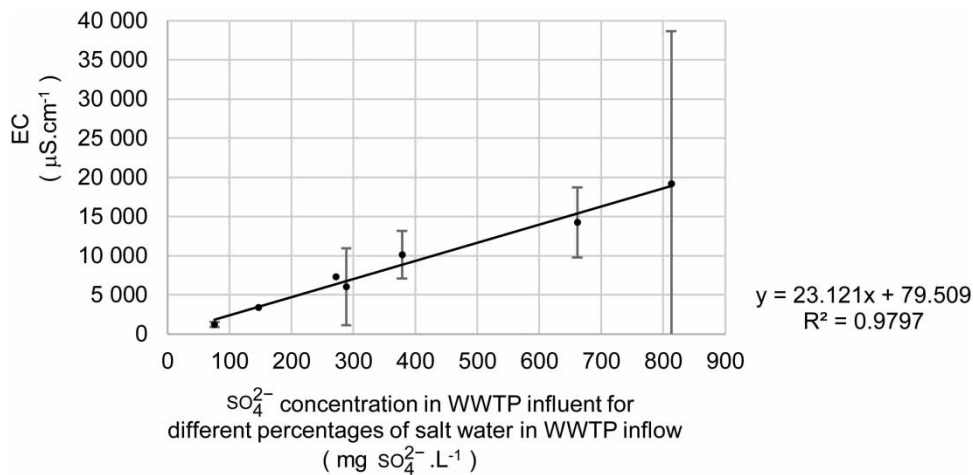


Figure 7 | Schematic for forecasting the model of volume of salt water and  $SO_4^{2-}$  load quantification based on high tide levels.



**Figure 8** | Correlation between EC and percentage of salt water in WWTP inflow.



**Figure 9** | Correlation between EC and SO<sub>4</sub><sup>2-</sup> concentration in WWTP influent.

**Table 2** | Assessment of the time series dataset for saltwater volume quantification

Month (2017)	Maximum high tide level m	Maximum instantaneous percentage of salt water in WWTP inflow (m <sup>3</sup> .min <sup>-1</sup> ) %	Estimated saltwater volume entering the wastewater collection system m <sup>3</sup>	Relative percentage to monthly WWTP inflow %
April	4.16	53.9	20,554	3.6
May	4.12	46.1	16,050	2.7
June	4.07	45.1	12,906	2.2
July	4.07	33.3	8,280	1.5

The mathematical expressions obtained make it possible to forecast the total monthly saltwater volume and SO<sub>4</sub><sup>2-</sup> load that will flow into the WWTP for the time periods covered by the high tide level values supplied by IH. Table 3 shows the monthly forecast for saltwater volume, and Table 4 for SO<sub>4</sub><sup>2-</sup> load.

The total monthly saltwater volumes estimated in Table 2 and the ones forecasted in Table 3 differ by 11.8% (April), 1.3% (May), 28.7% (June), and 1.3% (July), which is reasonably acceptable and promising. The larger differences arise from missing WWTP influent's EC data. Worth noticing is that weather conditions in the estuary might affect the local tide levels, and the

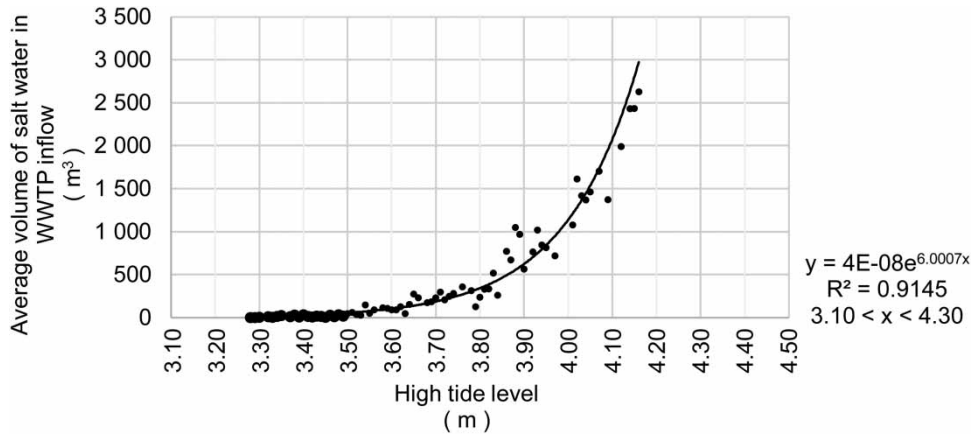


**Figure 10** | Scatterplot and exponential regression curve for the average volume of salt water for each high tide level.

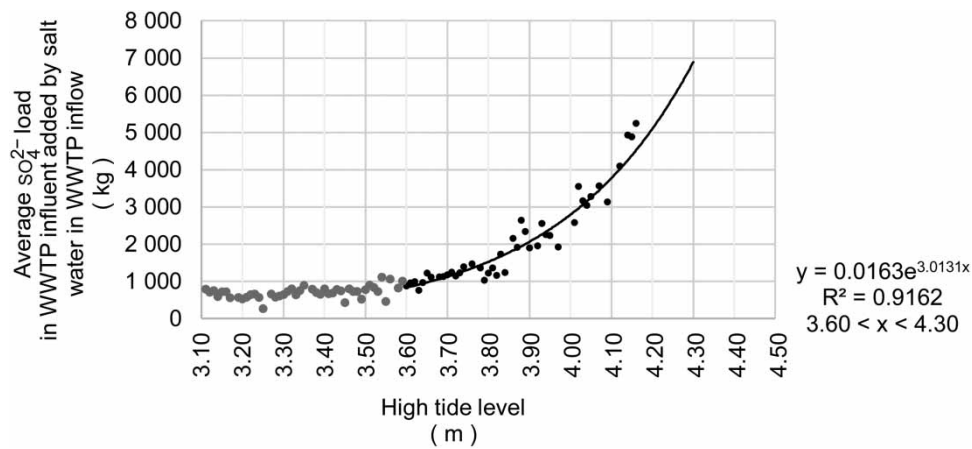


**Figure 11** | Scatterplot and exponential regression curve for the average  $SO_4^{2-}$  load for each high tide level.

**Table 3** | Monthly forecasts for the saltwater volume

2017			2018		
Month	Maximum high tide level m	Monthly forecast for saltwater volume from the Tagus Estuary m <sup>3</sup>	Month	Maximum high tide level m	Monthly forecast for saltwater volume from the Tagus Estuary m <sup>3</sup>
1	3.97	6,262	1	4.08	10,291
2	3.99	7,136	2	4.11	8,621
3	4.14	19,461	3	4.10	13,355
4	<b>4.16</b>	<b>22,988</b>	4	4.01	9,529
5	<b>4.12</b>	<b>15,837</b>	5	3.93	6,826
6	<b>4.07</b>	<b>9,196</b>	6	3.98	6,095
7	<b>4.07</b>	<b>8,132</b>	7	4.06	8,470
8	4.10	10,820	8	4.17	14,852
9	4.09	16,219	9	4.24	22,083
10	4.13	21,236	10	4.18	20,461
11	4.12	19,158	11	3.96	11,781
12	4.09	11,688	12	3.97	7,242
Maximum	4.16	22,988	Maximum	4.24	22,083
Total		168,133	Total		139,607

**Table 4** | Forecast monthly estimates from the model of sulfate load

2018		
Month	Maximum high tide level m	Forecast for the additional $\text{SO}_4^{2-}$ load from saltwater volume kg
1	4.08	46,212
2	4.11	37,794
3	4.10	54,889
4	4.01	49,008
5	3.93	43,221
6	3.98	37,381
7	4.06	41,580
8	4.17	52,729
9	4.24	64,339
10	4.18	66,902
11	3.96	54,968
12	3.97	43,580
Maximum	4.24	66,902
Total		592,603

timing of the high tide peak with the dilution effect generated by the WWTP's inflow regime (diurnal or nocturnal) can also contribute to minor deviations.

The forecasting capacity of these forecasting models will be more accurate with larger time series datasets. To maintain quality assurance some precautions should be taken, including regular verification and update, taking account of changes in the wastewater collection system network (e.g., corrective structural changes, aggravation of structural damage, and mean sea level rise).

## CONCLUSIONS

Saltwater intrusion into wastewater collection systems is a significant problem. It is generally accepted that the best strategy is mapping and assessing the wastewater collection system's critical sites and taking corrective actions. That can be very time-consuming and expensive for a water utility; however, other strategies might be suitable, such as forecasting models to support WWTP management team decision-making.

The forecasting models created show good correlation between both variables, average volume of salt water in WWTP inflow (0.9145) and average  $\text{SO}_4^{2-}$  load in WWTP influent added by the saltwater volume (0.9162), with the corresponding estuary's high tide levels. The models will be useful to WWTP management, with respect to both chemical dosing and process stability.

During the study, the highest monthly percentage of salt water in WWTP inflow, related to the monthly inflow, was 3.6%. While this might seem low, it is high enough to cause serious operating problems in the WWTP. On a shorter timescale, some critical situations were detected with elevated percentage of salt water in the WWTP inflow, the highest value being 53.9%, meaning that parts of the wastewater collection system and some pumping stations, briefly, transferred twice the supposed wastewater volume, with consequent increased energy consumption and operating costs. This problem is likely to be aggravated for coastal WWTPs due to mean sea level rise as the consequence of climate changes, and water utilities might need to find short-term adaptative strategies.

## ACKNOWLEDGEMENTS

The research was developed as part of a master's thesis (Figueiredo 2018) within the partnership between NOVA School of Science and Technology from NOVA University of Lisbon, and the water utility SIMARSUL (Saneamento da Península de

Setúbal, S.A.), a subsidiary company from the holding group Águas de Portugal, S.A. This research follows a previous work (Figueiredo *et al.* 2020) adding forecast models to quantify saltwater intrusion's volume and  $\text{SO}_4^{2-}$  load providing useful tools for WWTP management teams facing this problem.

## DATA AVAILABILITY STATEMENT

All relevant data are included in the paper or its Supplementary Information.

## REFERENCES

- Antunes, C. 2016 *Subida do nível médio do mar em Cascais, revisão da taxa actual (Mean sea Level Rise in Cascais, Rate Update Review)*. 4as Jornadas de Engenharia Hidrográfica, Lisboa, Portugal.
- APHA 1999 *Standard Methods for the Examination of Water and Wastewater*, 20th edn. American Public Health Association (APHA)/ American Water Works Association (AWWA)/Water Environment Federation (WEF), Singapore.
- Degrémont 1989 *Memento Technique de L'eau, Tome I et II (Water Treatment Handbook, Volumes I and II)*. Neuvième Édition. Lavoisier, Paris, France.
- Figueiredo, A. 2018 *Afluências indevidas de água salgada em ETAR. Medidas de quantificação e minimização. Caso de estudo ETAR do Barreiro/Moita (Undue Inflow of Saltwater in WWTP. Quantification and Mitigation Measures. Case Study of Barreiro/Moita's WWTP)*. M.Sc. thesis, Integrated Master's Degree in Environmental Engineering – Sanitary Engineering, NOVA School of Science and Technology, NOVA University of Lisbon, Lisbon, Portugal.
- Figueiredo, A., Amaral, A. & Pacheco, J. 2020 *Assessment for which tide level saltwater intrusion occurs in a sewer network. Case study: Barreiro/Moita WWTP, Portugal*. *Water Practice and Technology* **15** (3), 723–733.
- Firer, D., Friedler, E. & Lahav, O. 2008 *Control of sulfide in sewer systems by dosage of iron salts: comparison between theoretical and experimental results, and practical implications*. *Science of the Total Environment* **392**, 145–156.
- Instituto Hidrográfico (IH) (Hydrographic Institute). 2017 Available from: <http://www.hidrografico.pt/previsao-mares.php> (accessed 1 October 2017).
- McGhee, T. J. 1991 *Water Supply and Sewerage*, 6th edn. McGraw Hill, New York, USA.
- Metcalf & Eddy Inc. 2014 *Wastewater Engineering – Treatment and Resource Recovery*, 5th edn. McGraw-Hill Education, New York, USA.
- Phillips, J., Scott, C. & O'Neil, S. 2015 *Assessing the Vulnerability of Wastewater Facilities to sea-Level Rise King County Wastewater Treatment Division*, Vol. 3. King County Department of Natural Resources and Parks, Wastewater Division, Seattle, WA, USA, pp. 127–133.
- Serrano, C. 2014 *Impactes da presença de água do estuário do rio Tejo em ETAR. Caso de Estudo – ETAR do Seixal (Impact of Tagus River Estuary Saltwater Presence in WWTP Inflow. Case Study of Seixal's WWTP)*. M.Sc. thesis, Integrated Master's Degree in Environmental Engineering – Sanitary Engineering, NOVA School of Science and Technology, NOVA University of Lisbon, Lisbon, Portugal.
- Sistema Nacional de Informação de Recursos Hídricos (SNIRH) 2017 *(Water Resources National Information System)* website from Agência Portuguesa do Ambiente (APA) (Environmental Portuguese Agency). Available from: <https://snirh.apambiente.pt/> (accessed 1 October 2017).
- Talaiekhosani, A., Bagheri, M., Goli, A. & Khoozani, M. 2016 *An overview of principles of odor production, emission, and control methods in wastewater collection and treatment systems*. *Journal of Environmental Management* **170**, 186–206.
- Zhang, L., De Schryver, P., De Gussemé, B., De Muynck, W., Boon, N. & Verstraete, W. 2008 *Chemical and biological technologies for hydrogen sulfide emission control in sewer systems: a review*. *Water Research* **42**, 1–12.

First received 19 July 2021; accepted in revised form 23 September 2021. Available online 27 October 2021